

## Micro-flow-injection analysis (FIA) immunoassay of herbicide residue 2,6-dichlorobenzamide

towards automated at-line monitoring using modular microfluidics

**Uthuppu, Basil; Heiskanen, Arto; Kofoed, Dan; Aamand, Jens; Jørgensen, Claus; Dufva, Martin; Jakobsen, Mogens Havsteen**

*Published in:*  
Analyst

*DOI:*  
[10.1039/c4an01576b](https://doi.org/10.1039/c4an01576b)

*Publication date:*  
2015

*Document Version*  
Final published version

[Link to publication](#)

### *Citation (APA):*

Uthuppu, B., Heiskanen, A., Kofoed, D., Aamand, J., Jørgensen, C., Dufva, M., & Jakobsen, M. H. (2015). Micro-flow-injection analysis (FIA) immunoassay of herbicide residue 2,6-dichlorobenzamide: towards automated at-line monitoring using modular microfluidics. *Analyst*, 140(5), 1616-1623. DOI: 10.1039/c4an01576b

## DTU Library

Technical Information Center of Denmark

---

### General rights

Copyright and moral rights for the publications made accessible in the public portal are retained by the authors and/or other copyright owners and it is a condition of accessing publications that users recognise and abide by the legal requirements associated with these rights.

- Users may download and print one copy of any publication from the public portal for the purpose of private study or research.
- You may not further distribute the material or use it for any profit-making activity or commercial gain
- You may freely distribute the URL identifying the publication in the public portal

If you believe that this document breaches copyright please contact us providing details, and we will remove access to the work immediately and investigate your claim.



Cite this: *Analyst*, 2015, **140**, 1616

## Micro-flow-injection analysis ( $\mu$ FIA) immunoassay of herbicide residue 2,6-dichlorobenzamide – towards automated at-line monitoring using modular microfluidics†

Basil Uthuppu,\*<sup>a</sup> Arto Heiskanen,<sup>a</sup> Dan Kofoed,<sup>a</sup> Jens Aamand,<sup>b</sup> Claus Jørgensen,<sup>c</sup> Martin Dufva<sup>a</sup> and Mogens Havsteen Jakobsen<sup>a</sup>

As a part of developing new systems for continuously monitoring the presence of pesticides in ground-water, a microfluidic amperometric immunosensor was developed for detecting the herbicide residue 2,6-dichlorobenzamide (BAM) in water. A competitive immunosorbent assay served as the sensing mechanism and amperometry was applied for detection. Both the immunoreaction chip (IRC) and detection (D) unit are integrated on a modular microfluidic platform with in-built micro-flow-injection analysis ( $\mu$ FIA) function. The immunosorbent, immobilized in the channel of the IRC, was found to have high long-term stability and withstand many regeneration cycles, both of which are key requirements for systems utilized in continuous monitoring. The IRC was regenerated during 51 cycles in a heterogeneous competitive assay out of which 27 were without the analyte (the highest possible signal level) in order to assess the regeneration capability of the immunosorbent. Detection of BAM standard solutions was performed in the concentration range from  $62.5 \mu\text{g L}^{-1}$  to  $0.0008 \mu\text{g L}^{-1}$ . Non-linear regression of the data using the four-parameter logistic equation generated a sigmoidal standard curve showing an  $\text{IC}_{50}$  value (concentration that reduces the signal by 50%) of  $0.25 \mu\text{g L}^{-1}$ . The strongest signal variation is observed in the concentration range between 0.02 and  $2.5 \mu\text{g L}^{-1}$ , which includes the  $0.1 \mu\text{g L}^{-1}$  threshold limit set by the European Commission for BAM in drinking water. The presented results demonstrate the potential of the constructed  $\mu$ FIA immunosensor as an at-line monitoring system for controlling the quality of ground water supply.

Received 27th August 2014,  
Accepted 17th January 2015

DOI: 10.1039/c4an01576b

www.rsc.org/analyst

## Introduction

Immunoassays have been widely used in clinical chemistry<sup>1,2</sup> and endocrinology<sup>3</sup> since their emergence as an analytical tool in 1960.<sup>4</sup> In 1971, Ercegovich *et al.* presented immunoassays for DDT, malathion and aminotriazole, providing the first strong demonstration to environmental chemists on the potentials of immunoassays as an analytical technique suitable for

environmental monitoring.<sup>5</sup> Since then, immunoassays have found an increased acceptance in environmental analysis as also indicated by the growing number of publications in the field.<sup>6–10</sup> Immunoassays have many advantages over the widely used chromatographic methods, *e.g.*, cost-efficiency, throughput, simplicity and enhanced parallelisation. However, the concept of automated immunosensing has emerged as a part of system development for long-term monitoring of analytes. Along with expensive and complex centrifugal analysers and air-segmented continuous flow system,<sup>11</sup> flow-injection immunoanalysis (FIIA) systems have pioneered the development. The FIIA concept is a combination of batch-based immunoassay and flow-injection analysis (FIA) methodology originally described by Ruzicka and Hansen in 1975.<sup>12</sup> The strength and simplicity of FIA are based on the easily controllable and reproducible sample introduction and dispersion in an unsegmented continuously flowing carrier stream. A comprehensive review on FIIA applications using various immunoanalysis formats can be found in literature.<sup>13</sup> Most of the

<sup>a</sup>Department of Micro- and Nanotechnology, Technical University of Denmark, Ørstedes Plads, Bygning 345Ø, 2800 Kgs. Lyngby, Denmark.  
E-mail: baut@nanotech.dtu.dk

<sup>b</sup>The Geological Survey of Denmark and Greenland (GEUS), Oester Voldgade 10, 1350 Copenhagen, Denmark

<sup>c</sup>DHI Water & Environment, Agern Allé 5, 2970 Hørsholm, Denmark

†Electronic supplementary information (ESI) available: Fully automated amperometric BAM immunosensor; Design and fabrication of different modules of BAM immunosensor; The cascade of fluidic operations during immunosorbent regeneration and generation of the standard curve. See DOI: 10.1039/c4an01576b

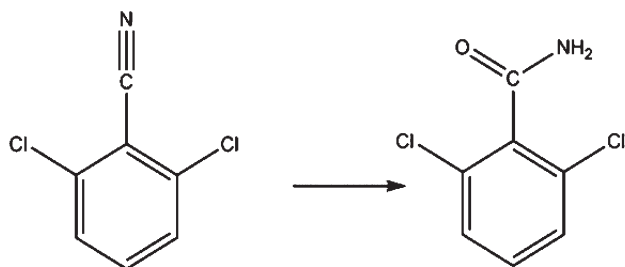


Fig. 1 Chemical structure of dichlobenil and its main metabolite 2,6-dichlorobenzamide (BAM).

reported amperometric FIA applications employ a reaction column for the immunoreaction step whereas the detection is performed by coupling a separate amperometric detector with a commercially available FIA system.<sup>14–17</sup>

BAM is the main metabolite of the widely used herbicide, dichlobenil (Fig. 1).<sup>18</sup> It is more persistent, more mobile and water soluble than dichlobenil. Hence, it may reach natural water resources more effectively. Toxicity studies indicate that consumption of a few hundred  $\text{mg kg}^{-1}$  of BAM can cause acute toxicity in mammals.<sup>19</sup> In Denmark where the entire drinking water supply is based on groundwater,<sup>20</sup> studies conducted by the Danish groundwater monitoring programme revealed that 25% of water supply wells contain BAM and 10% exceed the European Commission threshold limit of  $0.1 \mu\text{g L}^{-1}$  for pesticides in drinking water.<sup>21</sup> Bruun *et al.* have presented a heterogeneous labelled competitive immunoassay for BAM analysis in water.<sup>22</sup> It is highly specific and sensitive as well as much simpler and cost-effective in terms of the necessary

sample pre-treatment and instrumentation than the conventional chromatography based techniques.<sup>23</sup> In the competitive format, the free BAM in a water sample inhibits the binding of the horseradish peroxidase (HRP) labelled anti-BAM monoclonal antibody (HYB 273) onto the immunosorbent, which is the immobilized BAM hapten. The concentration of the surface bound antibody (inversely proportional to the concentration of BAM in a sample) is then detected by the peroxidase reaction of 3,3',5,5'-tetramethylbenzidine (TMB) substrate which is both optically and electrochemically active.<sup>24,25</sup> In microtitre plate format, the developed assay is suitable for extensive parallelisation. However, transfer into a serial FIA environment requires that the immunosorbent be able to withstand multiple regeneration cycles. We have therefore previously optimized the immunosorbent of the original microtitre plate assay to enhance regeneration efficiency using glycine hydrochloride regeneration solution.<sup>26</sup>

Here, we present the development and fabrication of an automated amperometric immunosensor for BAM monitoring based on the FIA concept implemented as a modular microfluidic flow-injection analysis ( $\mu\text{FIA}$ ) system, comprising all the necessary modules and functions (Fig. 2 and S-1†): (1) fluidic control with Labview programmable multichannel micropump and valves, (2) reagent reservoirs, (3) immunoreaction chip (IRC), (4) solution mixing chip (MC), and (5) detection (D) unit. We demonstrate the achieved regeneration efficiency of our previously developed modified immunosorbent and its suitability for  $\mu\text{FIA}$  environment. The system provides significant cost-effectiveness as well as functional and operational potential, paving the way for implementation of autonomous, compact at-line immunosensor systems for monitoring water safety.

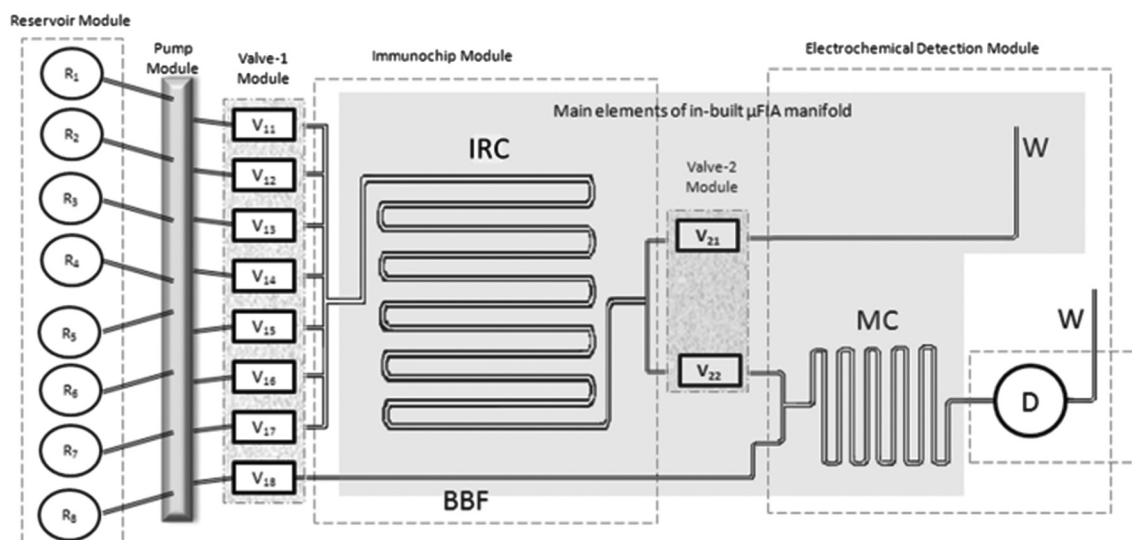


Fig. 2 A Schematic representation of  $\mu\text{FIA}$  BAM immunosensor constructed by interconnecting individual modules to facilitate different functions: Reagent reservoirs (R1 to R8) for different solutions to be delivered sequentially into the immunoreaction chip (IRC). The fluidic operations are controlled by the miniaturized peristaltic micropump automated by LEGO® servo motors and valves (module 1: V11 to V18; module 2: V21 and V22). During assays, V18 provides a continuous flow of baseline buffer (BBF) from R8 through the mixing chip (MC) to the detection unit (D). After immunoreaction, the contents of the channel in IRC are flushed either to the waste (W) or to D for detection using valves V21 and V22. During detection, the electrochemically active substrate is mixed with BBF in MC and directed further to D where the amperometric peaks are recorded.

## Experimental

### Materials

Poly(methyl methacrylate) (PMMA) (Röchling Technische Teile KG, Mainburg, Germany), Polycarbonate (PC) (Bayer Material Science AG, Leverkusen, Germany), and polydimethylsiloxane (PDMS) made of Sylgard® 184 silicone elastomer kit (Dow Corning, Wiesbaden, Germany) were used for fabrication and interfacing of microfluidic components.

### Chemicals

Anti-BAM monoclonal antibody (HYB 273) was provided by Statens Serum Institut, Copenhagen, Denmark. Horseradish peroxidase (HRP) (EZ-Link® Plus Activated Peroxidase) was purchased from Pierce (Rockford, IL, USA) and conjugated with HYB 273 at pH 7.2 according to the procedure given by the supplier. Ready-to-use TMB-Plus substrate (3,3',5,5'-tetramethylbenzidine) was from Kem-En-Tec Diagnostics A/S (Taastrup, Denmark). 2,6-Dichlorobenzamide (BAM) (10 mg mL<sup>-1</sup> in acetonitrile) standard reference was purchased from Dr Ehrenstorfer GmbH (Augsburg, Germany). Phosphate buffered saline (PBS) powder in pouches, potassium chloride (KCl), glycine hydrochloride (Gly-HCl), PBS with Tween® 20 tablets, potassium hexacyanoferrate(III) (K<sub>3</sub>Fe(CN)<sub>6</sub>) were from Sigma-Aldrich Corporation (St. Louis, MO, USA).

### Buffers and standard solutions

All solutions were prepared using ultra-pure water (resistivity 18.2 MΩ cm) from a Milli-Q® water purification system (Millipore Corporation, Billerica, MA, USA). Dissolving one pouch of PBS powder in 1 L of Milli-Q water yielded 0.01 M PBS of pH 7.4 (containing 0.14 M NaCl and 0.0027 M KCl) which was used as the baseline buffer. The assay buffer was prepared by dissolving one tablet of PBS with Tween® 20 in 500 mL of Milli-Q water which yielded 0.01 M PBS of pH of 7.4 containing 0.05% Tween® 20 (PBST). The regeneration buffer was prepared by dissolving 1.12 g of Gly-HCl in 100 mL of Milli-Q® water (100 mM) and the pH was adjusted to 2. BAM standard solutions were prepared by adding the standard reference BAM in acetonitrile in Milli-Q® water to obtain a dilution series with the following concentrations (in µg L<sup>-1</sup>): 62.5, 12.5, 2.5, 0.5, 0.1, 0.02, 0.004, and 0.0008.

### Instrumentation

Hapten immobilization in the micro-channels was done using a UV Stratalinker® 2400 UV reaction chamber from Stratagene (La Jolla, CA, USA). All parts of the microfluidic system were fabricated using Computer Numerical Control (CNC) micro-milling machine (Folken Industries, Glendale, California) and a Mini-Mill/3Pro software (Minitech Machinery Corporation, Norcross, GA, USA) which executes G-code generated by EZ-CAM15 Express software (EZCAM Solutions, Inc., New York, NY, USA). UV-activated thermal bonding of the microfluidic chips was done using 5000-EC Series UV Curing Flood Lamp System (Dymax Corporation, Torrington, CT, USA) and a PW20 hydraulic press (Paul-Otto Weber GmbH, Remshalden,

Germany). Screen printed carbon electrodes (DRP-110) for the amperometric detection unit were purchased from DropSens (Oviedo, Spain). Cyclic voltammetric and amperometric experiments were performed using a computer controlled 8-channel CHI1010A potentiostat (CH Instruments, Inc., Austin, TX, USA). Miniaturized pump and valves were operated with Lego® Interactive Servo Motors (Lego System A/S, Billund, Denmark) that were controlled by an NXT Intelligent Brick (Lego System A/S, Billund, Denmark) executing a LabView-based script. Mettler-Toledo SevenEasy pH meter S 20 (Mettler-Toledo AG, Schwerzenbach, Switzerland) was used to determine pH in the different solutions.

### Construction of modular microfluidic platform with in-built µFIA function

The microfluidic platform for the amperometric µFIA BAM immunosensor has a baseplate (fabricated of PC) comprising the various modules to facilitate the necessary functions, such as programmable fluidic operations (miniaturized 8-channel peristaltic micropump and 8-channel valves), solution supply and mixing, immunoreaction, as well as amperometric detection. Details of the structure and fabrication of these modules can be found in the ESI (S-2).† The interconnections between the modules of the entire system were formed using PDMS-based ball joint interconnection blocks (BJIB) and pump ribbons previously described elsewhere.<sup>27</sup> The fabrication and characterization of the peristaltic micropump and valves, as well as their automation using the programmable Lego® Interactive Servo Motors have been previously presented by Sabourin *et al.*<sup>28</sup>

The schematic representation of the µFIA BAM immunosensor (Fig. 2) shows how the various modules are interconnected and placed on the microfluidic platform. The different solutions from the reservoir module (R<sub>1</sub>...R<sub>8</sub>) are sequentially delivered into the immunoreaction chip (IRC). Valve module 1 (V<sub>11</sub>...V<sub>18</sub>) is used to select the reagent reservoir (R<sub>11</sub>...R<sub>18</sub>; made of PC). The washing solutions are directed to the waste (W) using valve module 2 (V<sub>21</sub> and V<sub>22</sub>). During detection, the microfluidic channel of the IRC (made of PMMA) functions as the injection loop of the µFIA system, containing the electrochemically active substrate. The solution from the IRC is then mixed with an uninterrupted flow of the baseline buffer (BBF) on the mixing chip (MC; made of PMMA) using valve module 2 and directed further to the detection unit (D; made of PMMA) for recording the current signals.

During all fluidic operations, the LEGO® motor was set to provide a flow rate of 30.0 ± 0.2 µL min<sup>-1</sup>, which is the approximate volume of the microchannel in IRC loop and detection chamber in D.

### Evaluation of the µFIA function

The in-built µFIA function was evaluated by amperometric detection using solutions having a varying concentration of K<sub>3</sub>[Fe(CN)<sub>6</sub>] (in mM: 10, 5, 2.5, 1.25, and 0.625) in PBS. The channel in IRC (µFIA injection loop) was filled with K<sub>3</sub>[Fe(CN)<sub>6</sub>] solution from reservoir R4 and eluted by PBS from reservoir R5

into the continuous baseline buffer stream from reservoir R8 and further to D for detection. The miniaturized peristaltic micropump and valves (modules 1 and 2) were used to control the above described fluid delivery steps. The working electrode was poised at  $-200$  mV vs. the Ag/AgCl reference electrode (RE). The reduction current was recorded as a function of time. The area under the recorded current peaks (five repetitions for each concentration) was plotted as a function of concentration. The error bars represent average  $\pm$  standard deviation. All the measurements were performed at room temperature.

### Immunosorbent and its regeneration

The immunosorbent was prepared by immobilizing the optimized BAM hapten (hapt D, described in ref. 26) in the microchannel of IRC. The hapt D solution ( $10 \mu\text{g L}^{-1}$ ; 1:100 dilution of stock solution in PBS) was introduced into the channel using a syringe. The covalent immobilization of the hapten onto the channel surface was achieved under 30 min UV exposure. After assembling the IRC onto the microfluidic platform, the channel was washed with PBST for 5 min. After each cycle of immunoreaction, the immunosorbent was regenerated by incubating (stop flow) with 100 mM Gly-HCl solution for 5 min followed by a washing with PBST.

The robustness of the immunosorbent to withstand repeated regeneration (stripping off the bound antibody from the immunosorbent) cycles was tested by performing the immunoreaction and regeneration 27 times (12 times with spectrophotometric detection at 625 nm and 15 times with amperometric detection). In both cases the immunoreaction was conducted without free BAM in solution to obtain the highest possible signal and surface coverage by the used antibody concentration. The HYB 273 antibody stock solution ( $\sim 1$  mg  $\text{mL}^{-1}$ ) was diluted 1:100 in PBST. 150  $\mu\text{L}$  of this working solution was mixed with 50  $\mu\text{L}$  of Milli-Q water. The removal of surface bound antibody after regeneration was evaluated by conducting substrate ( $\text{TMB}_{\text{red}}$ ) reaction (40 min) followed by recording of the corresponding current signal generated by reduction of the oxidised substrate ( $\text{TMB}_{\text{ox}}$ ) detected at  $-100$  mV vs. the Ag/AgCl RE. All the experimental steps were performed at room temperature.

Cyclic voltammetry of the commercially available TMB substrate ( $\text{TMB}_{\text{red}}$ ) and its HRP-oxidized product ( $\text{TMB}_{\text{ox}}$ ) was used to determine the appropriate potential for amperometric detection. Both solutions ( $\text{TMB}_{\text{red}}$  and  $\text{TMB}_{\text{ox}}$ ) were prepared by mixing with PBS in 1:1 ratio and pumped into the detection chamber (D). The cyclic voltammogram (CV) of  $\text{TMB}_{\text{ox}}$  was recorded 40 min after addition of HRP in the TMB solution (final HRP concentration of 125 pM).

### Generation of standard curve

A standard curve (concentration response) was generated by using standard solutions having known concentrations of BAM during the immunoreaction in IRC. The same immunosorbent was used throughout the experimental procedures including the regeneration tests described above. The sigmoidal

curve (charge vs. concentration on logarithmic scale) was plotted and fitted to the four-parameter logistic equation using non-linear regression (GraphPad Prism version 6.0 for Windows from GraphPad Software, Inc., La Jolla, CA, USA) to obtain the  $\text{IC}_{50}$  (the effective concentration of BAM that reduces the signal by 50%). The approximate linear working range was determined from the standard curve and compared with that obtained using ELISA.<sup>22</sup> 150  $\mu\text{L}$  of the HYB 273 antibody working solution (prepared as described above) was mixed with 50  $\mu\text{L}$  of the different BAM standard solutions. Mixing of each solution was done in one of the reservoirs 15 min before introducing it into the IRC for immunoreaction. Details describing the cascade of fluidic operations during generation of the standard curve are provided in the ESI (S-3).<sup>†</sup> The cycle of immunoreaction and immunosorbent regeneration was repeated at least three times for each BAM concentration. The area of the obtained amperometric peaks is directly proportional to the concentration of formed  $\text{TMB}_{\text{ox}}$ , which, in turn, is inversely proportional to the concentration of the BAM that competes for the antibody (HYB 273) with the surface immobilized BAM hapten (hapt D).

## Results and discussion

### Fabrication of $\mu\text{FIA}$ based amperometric immunosensor

Fabrication of the  $\mu\text{FIA}$  BAM immunosensor platform (ESI S-2<sup>†</sup>), comprising the baseplate and the different modules, was achieved using fast prototyping techniques, such as micromilling and UV assisted thermal bonding. Use of polymers (PC, PMMA, and PDMS) facilitated construction of a simple, cost-effective, reproducibly functioning, and user friendly system. PMMA, used for fabricating the main modules of the system, has low hydrophobicity and can be easily modified.<sup>29</sup> Most importantly, it is sufficiently UV permeable to allow the hapten immobilization. Elasticity of PDMS<sup>30</sup> has been instrumental in achieving the functionality of the ribbons used in the micropump and valves as well as leakage-proof sealing to flat surfaces using the BJIB module-to-module interconnections.<sup>27</sup> The known disadvantage of PDMS, *i.e.*, its ability to adsorb different molecules, especially proteins,<sup>31</sup> was minimised in this application using the assay buffer that contains the non-ionic surfactant Tween@20.

The modular structure provides several advantages, *e.g.*, fabrication simplicity, easy component integration and interchangeability, as well as easy automation and maintenance. The assembly of the different modules on the baseplate (as well as disassembly during maintenance) is simplified by the 'plug-in' interconnection features, *i.e.* the combination of BJIBs at both ends of the PDMS ribbons and the complementary 8-hole arrays at interfaces of each module.

The central feature of the system is the in-built micro-flow-injection analysis ( $\mu\text{FIA}$ ) function schematically shown in Fig. 2. Valve module 2 routes the immunoreaction solution from the microchannel of IRC to either the mixing chip (MC) or the waste (W). The constructed valving makes the micro-



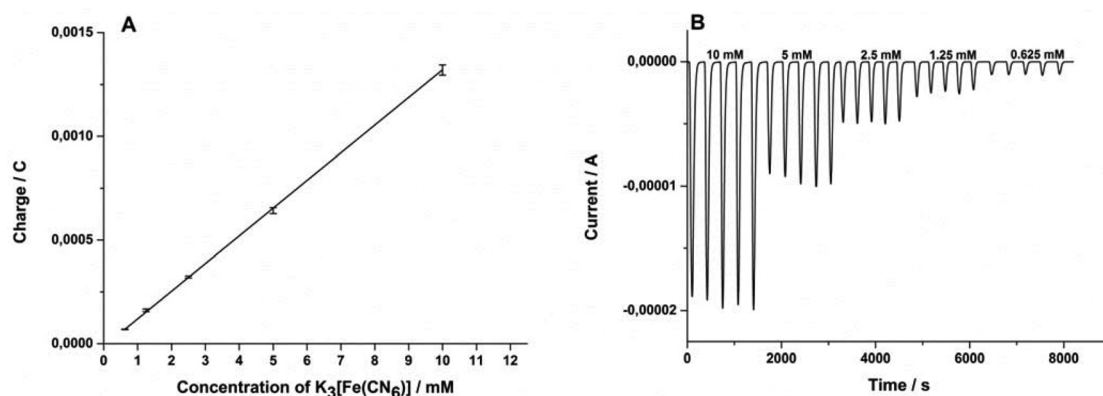


Fig. 3 (A) The linear relationship between the average peak areas in the amperometric recordings and concentration of  $K_3[Fe(CN)_6]$  injected into the detection chamber from the microchannel of IRC (injection loop) of the  $\mu$ FIA system. Five injections were made for each concentration; the error bars represent standard deviation. (B) A set of recorded reduction current peaks for each of the used concentration of  $K_3[Fe(CN)_6]$  (in mM: 10, 5, 2.5, 1.25, and 0.625).

channel function as an effective injection loop. The baseline buffer (BBF), continuously fed into the MC and further to the detection chamber (D), provides the background signal. The injection of the reacted substrate into the continuous BBF stream is done using a carrier buffer with the same composition but originating from a different reservoir. Diffusive mixing of the plug of the reacted substrate with the BBF (generating the recorded background signal) is facilitated by the narrow long mixing channel. Unlike in conventional FIA, in our  $\mu$ FIA system, mixing of the reactive sample plug from the loop with BBF introduces a dilution factor. However, due to the well-controlled mixing, the obtained output signal is reproducibly reflecting the concentration of the electroactive substance in the loop. Another advantage of the design is that during an immunoassay the used reagents and washing solutions are routed to the waste using valve module 2, minimizing the effect of electrode fouling on the recorded signal. Amperometry as the used detection technique facilitated construction of an easily integrated compact detection unit.

The  $\mu$ FIA function also allowed minimization of reagent quantities, significantly reducing the overall reagent consumption, which contributed to low operational costs. For instance, one complete immunoassay, as described in the Experimental section and in the ESI (S-3),† required approximately 30 ng of antibody. This is roughly 500 times lower compared to the amount needed for a corresponding ELISA-based assay in a 96-well microtitre plate.

#### Characterization of the $\mu$ FIA function

The  $\mu$ FIA function was evaluated by amperometric recording of the reduction current upon injection of  $K_3[Fe(CN)_6]$  samples in the concentration range between 0.625 and 10 mM. As shown in Fig. 3A, the area of the recorded peaks (the total charge associated with the reduction) varies linearly with respect to concentration ( $R^2 = 0.9995$ ). Each data point represents the average charge generated in five repeated injections of the same concentration and the error bars indicate the stan-

dard deviation. Fig. 3B shows the individual peaks, the area of which varied less than 5%. The well-defined peaks and their reproducibility result from the accuracy of the  $\mu$ FIA function, which provides: (1) a constant flow rate, (2) smooth switching between the loading and injection mode using the valves, and (3) effective mixing of the baseline buffer with the introduced electroactive substances in the microchannel of the MC. Consistency in achieving a constant baseline after each recorded peak demonstrates the precise fluidic operations facilitated by the module-to-module interconnections that minimize void volumes.

#### Characterization of BAM immunosensor

From the CVs shown in Fig. 4,  $-100$  mV vs. Ag/AgCl RE was chosen as the applied potential for amperometric detection of  $TMB_{ox}$  during the immunoassay cycles for both assessment of the degree of regeneration and calibration. The CVs are consistent with those presented previously in literature.<sup>25,32</sup> The applied potential provides a sufficient driving force for the

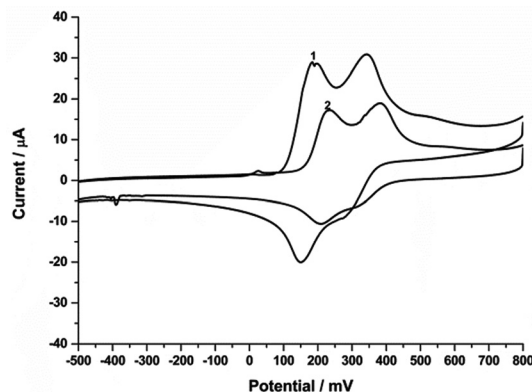


Fig. 4 Cyclic voltammograms of TMB (1) and oxidized TMB (2). The scan rate was 50 mV s<sup>-1</sup> and 0.01 M PBS was added as counter electrolyte. The potentials were adjusted vs. Ag/AgCl RE.

reduction of  $\text{TMB}_{\text{ox}}$  without any interfering cathodic processes.

In the regeneration assessment, the immunoassay steps were performed repeatedly without added BAM (zero BAM) in the solution. This allowed evaluation of the regeneration efficiency under the same reaction conditions as during actual immunoassays in the presence of BAM while being able to generate the maximal signal. The microchannel of IRC was regenerated 27 times. The regeneration experiments aimed at establishing the feasibility of performing BAM immunoassay for a number of times without losing the immunosorbent reactivity, which is considered to be a very important prerequisite in the development of an at-line monitoring system based on immunoassay. The results obtained in this series of experiments are shown in Fig. 5.

The fluctuations in the determined relative signal strength can be caused by, for instance, changes in the ambient temperature that can influence the temperature sensitive enzymatic reaction between each cycle. However, the observed overall reduction in the relative signal strength (<10% based on the slope of the linear fit) after a number of regenerations indicate that the immunosorbent was robust. This corroborates our previous findings demonstrating that surfaces with immobilized hapt D are better in terms of regeneration efficiency<sup>26</sup> than those having the hapten used in the original BAM immunoassay described by Bruun *et al.*<sup>22</sup> Along with the optimised immunochemistry, the microfluidic environment in the BAM immunosensor helped, to a great extent, satisfy the above mentioned requirement of at-line monitoring. The increased surface to volume ratio in the microchannel of IRC enhanced the interaction of the immunosorbent surface with the reagents in the fluid flow by decreasing the diffusion distance. Such conditions are equally beneficial for both sorption and desorption of the complexes formed between the antibody and the surface immobilized antigen. During the substrate reactions conducted immediately after regeneration of immuno-

sorbent, small peaks were obtained. However, the peak areas were negligible in comparison with the ones obtained during immunoassays. These small peaks were possibly a consequence of the commercial TMB substrate whose chemical composition is not fully known. However, there were no reduction peaks indicating the formation of  $\text{TMB}_{\text{ox}}$  during the substrate reaction, which reflects the efficiency of the antibody stripping during regeneration of the immunosorbent under the relatively mild conditions (stopped flow for 5 minutes during exposure to 100 mM Gly-HCl). Additional tests, using IRCs after storage for a couple of months at dry conditions, indicated that the immunosorbent retained almost 90% of its activity. The same IRC was also used for generating the standard curve at varying BAM concentrations from zero to  $62.5 \mu\text{g L}^{-1}$  with 3 repetitions for each concentration, thus, resulting in 51 regeneration cycles altogether.

Fig. 6 shows the generated sigmoidal standard curve (peak area vs. concentration on a logarithmic scale) based on the performed immunoreactions upon introduction of the different BAM concentrations in the range from  $62.5$  to  $0.0008 \mu\text{g L}^{-1}$ . An  $\text{IC}_{50}$  value (concentration that reduces the signal by 50%) of  $0.25 \mu\text{g L}^{-1}$  was obtained based the curve fitting. A significant (measurable) signal variation is observed in the concentration range between  $0.02$  and  $2.5 \mu\text{g L}^{-1}$ , which roughly coincides with the linear part of the sigmoidal fitted curve, which includes the threshold limit set by the European Commission for BAM ( $0.1 \mu\text{g L}^{-1}$ ) in drinking water.

The higher  $\text{IC}_{50}$  compared to the value obtained in the original microtitre plate based assay ( $0.19 \mu\text{g L}^{-1}$ ) indicates the reduced interaction between the antibody and the optimised immunosorbent. However, this weak interaction facilitated the effective regeneration of the immunosorbent. The observed variation of each point on the curve reflects the discrepancies associated with the automation of the sensor which has a great influence on the enzymatic reaction (signal recording step). Unlike the microtitre plate based assay, no end point

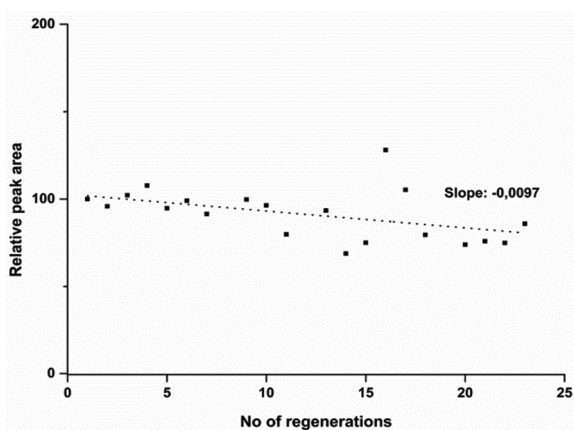


Fig. 5 Relative peak area after a number of repeated regeneration cycles (comparison with respect to the initial peak area). The dotted line shows the linear fit of the scatter plot.

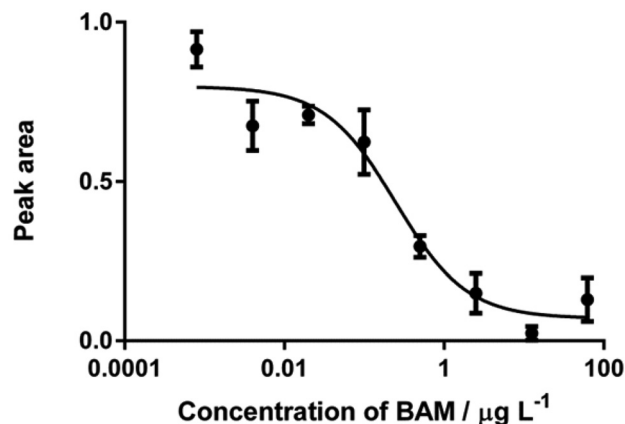


Fig. 6 A sigmoidal standard concentration response curve generated using 2,6-dichlorobenzamide (BAM) standards solutions in the concentration range from  $62.5$  to  $0.0008 \mu\text{g L}^{-1}$  (three repetitions for each concentration). The error bars represent standard deviation. The obtained  $\text{IC}_{50}$  value is  $0.25 \mu\text{g L}^{-1}$ .

detection by adding an acid to stop the enzymatic reaction with the substrate is adopted in this case. As a result, very small differences in the operation of the valve that directs the reacted substrate into the detection chamber may lead to significant variations in the signal recorded during consecutive assay cycles. Also, the current design of the reservoir module does not provide separate chambers for different (premixed) antibody-BAM standard solutions. The use of a single reservoir for all the standards required prolonged washing steps to avoid memory effects after each analytical cycle. This factor also influenced the reproducibility of the collected data. However, the presented results demonstrate the efficiency of the immunosorbent regeneration and the capability of the  $\mu$ FIA immunosensor to function in at-line monitoring of groundwater supply.

## Conclusions

As a part of developing new at-line sensor systems to monitor pesticide residues in groundwater, an immunosensor prototype was constructed on a microfluidic platform for 2,6-dichlorobenzamide (BAM) analysis using amperometric detection. The platform has a modular structure, which makes it simple and cost-effective to construct as well as easy to automate and maintain. The in-built micro-flow-injection analysis ( $\mu$ FIA) function, operated by the programmable fluid delivery system (peristaltic micropump and valves), combined with the effective module-to-module interconnections provides nearly 1:500 reduction in reagent consumption in comparison with conventional ELISA-based assays. The robustness and reusability of the immunosorbent was proved by repeatedly regenerating the microfluidic channel surface where the hapten is immobilized. Non-linear regression based fitting of immunoassay data to the four-parameter logistic equation generated a standard curve with an  $IC_{50}$  value of  $0.25 \mu\text{g L}^{-1}$ . The strongest signal variation (highest sensitivity) was observed in the concentration range between  $0.02 \mu\text{g L}^{-1}$  and  $2.5 \mu\text{g L}^{-1}$ . This shows the potential of the system in further development of at-line analysis systems for control of ground water quality considering the  $0.1 \mu\text{g L}^{-1}$  threshold as the maximum admissible concentration of BAM.

This proof of concept prototype can be instrumental to develop tailor-made sensors systems for various environmentally significant analytes. The modularity of the presented microfluidic platform, here demonstrated in BAM analysis, offers the possibility of constructing different systems for different applications by merely interchanging the order of various modules. Having an automated in-built  $\mu$ FIA function makes the system unique and facilitates easy integration with sensitive detection schemes. However, for further enhancing the analytical precision, improvements in the system engineering and automation are required. Currently, attempts are ongoing to use more precise stepper motors instead of Lego servomotors for controlling the miniaturised pumps and valves.

## Acknowledgements

We acknowledge the Fluidic Array Systems and Technology (FAST) group members, especially Dr David Sabourin and Alvaro José Conde for sharing the MainSTREAM platform technology. We also thank Per Thor Jonassen for his advice in the micromilling.

This work was co-funded by the following projects: (1) Sensors for monitoring and control of water quality, SENSO-WAQ, from the Danish Agency for Science, Technology and Innovation (grant no. 2104-06-000), (2) Reuse of water in the food and bioprocessing industries, REWARD, from the Danish Council for Strategic Research (grant no. 1308-00027B), (3) Mælkeafgiftsfonden (c/o Landbrug & Fødevarer Agro Food, Park 13, DK-8200 Århus N), and (4) The joint KAIST-DTU signature project, INTEGRATED WATER TECHNOLOGY.

## Notes and references

- 1 R. L. Searcy, J. V. P. Carroll, J. S. Carlucci and L. M. B. quist, *Clin. Chem.*, 1962, **8**, 166–171.
- 2 B. C. D. Villano, S. Brennan, P. Brock, C. Bucher, V. Liu, M. McClure, B. Rake, S. Space, B. Westrick, H. Schoemaker and J. V. R. Zurawski, *Clin. Chem.*, 1983, **29**, 549–552.
- 3 S. R. Nussbaum, R. J. Zahradnik, J. R. Lavigne, G. L. Brennan, K. Nozawa-Ung, L. Y. Kim, H. T. Keutmann, C. A. Wang, J. J. T. Potts and G. V. Segre, *Clin. Chem.*, 1987, **33**, 1364–1367.
- 4 R. S. Yalow and S. A. Berson, *J. Clin. Invest.*, 1960, **39**, 1157–1175.
- 5 C. D. Ercegovich, *Adv. Chem. Ser.*, 1971, **104**, 162–177.
- 6 R. L. T. Churchill, C. Sheedy, K. Y. F. Yau and J. C. Hall, *Anal. Chim. Acta*, 2002, **468**, 185–197.
- 7 M.-C. Hennion and D. Barcelo, *Anal. Chim. Acta*, 1998, **362**, 3–34.
- 8 G. Jay and B. Svetlana, *Analysis of Pesticides in Food and Environmental Samples*, CRC Press, Taylor & Francis Group, Boca Raton, ch. 9.
- 9 E. P. Meulenberg, W. H. Mulder and P. G. Stoks, *Environ. Sci. Technol.*, 1995, **29**, 553–561.
- 10 V. S. Morozova, A. I. Levashova and S. A. Eremin, *J. Anal. Chem.*, 2005, **60**, 202–217.
- 11 S. Daunert, L. G. Bachas, G. S. Ashcom and M. E. Meyerhoff, *Anal. Chem.*, 1990, **62**, 314–318.
- 12 J. Ruzicka and E. H. Hansen, *Flow Injection Analysis*, A Wiley-Interscience publication, New York, 2nd edn, 1998.
- 13 R. Puchades, A. Maquieira and J. Atienza, *Crit. Rev. Anal. Chem.*, 1992, **23**, 301–321.
- 14 W. U. De Alwis, B. S. Hill, B. I. Meiklejohn and G. S. Wilson, *Anal. Chem.*, 1987, **59**, 2688–2691.
- 15 B. B. Dzantiev, A. V. Zherdev, M. F. Yulaev, R. A. Sitdikov, N. M. Dmitrieva and I. Y. Moreva, *Biosens. Bioelectron.*, 1996, **11**, 179–185.
- 16 D. A. Palmer, T. E. Edmonds and N. J. Seare, *Analyst*, 1992, **117**, 1679–1682.
- 17 M. Stiene and U. Bilitewski, *Analyst*, 1997, **122**, 155–159.



- 18 M. S. Holtze, H. C. B. Hansen, R. K. Juhler, J. Sørensen and J. Aamand, *Environ. Pollut.*, 2007, **148**, 343–351.
- 19 E. Bjorklund, B. Styrihave, G. G. Anskjaer, M. Hansen and B. Halling-Soerensen, *Sci. Total Environ.*, 2011, **409**, 3732–3739.
- 20 C. Martínez Navarrete, J. Grima Olmedo, J. Durán Valsero, J. Gómez Gómez, J. Luque Espinar and J. de la Orden Gómez, *Environ. Geol.*, 2008, **54**, 537–549.
- 21 Council Directive 98/83/EC of 3 November 1998 on the quality of water intended for human consumption, *Official Journal of the European Communities*, 1998, L 330/32-L 330/54.
- 22 L. Bruun, C. Koch, B. Pedersen, M. H. Jakobsen and J. Aamand, *J. Immunol. Methods*, 2000, **240**, 133–142.
- 23 E. Bjorklund, G. G. Anskjaer, M. Hansen, B. Styrihave and B. Halling-Soerensen, *Sci. Total Environ.*, 2011, **409**, 2343–2356.
- 24 P. Fanjul-Bolado, M. B. González-García and A. Costa-García, *Anal. Bioanal. Chem.*, 2005, **382**, 297–302.
- 25 G. Liu, S. L. Riechers, C. Timchalk and Y. Lin, *Electrochem. Commun.*, 2005, **7**, 1463–1470.
- 26 B. Uthuppu, J. Aamand, C. Jørgensen, S. M. Kiersgaard, N. Kostesha and M. H. Jakobsen, *Anal. Chim. Acta*, 2012, **748**, 95–103.
- 27 D. Sabourin, D. Snakenborg and M. Dufva, *Microfluid. Nanofluid.*, 2010, **9**, 87–93.
- 28 D. Sabourin, P. Skafte, M. J. Søre, M. Hemmingsen, M. Alberti, V. Coman, J. Petersen, J. Emnéus, J. P. Kutter, D. Snakenborg, F. Jørgensen, C. Clausen, K. Holmstrøm and M. Dufva, *J. Lab. Autom.*, 2013, **18**, 212–228.
- 29 Y. Chen, L. Zhang and G. Chen, *Electrophoresis*, 2008, **29**, 1801–1814.
- 30 W. K. T. Coltro, S. M. Lunte and E. Carrilho, *Electrophoresis*, 2008, **29**, 4928–4937.
- 31 B. Huang, H. K. Wu, S. Kim and R. N. Zare, *Lab Chip*, 2005, **5**, 1005–1007.
- 32 G. Volpe, D. Compagnone, R. Draisci and G. Palleschi, *Analyst*, 1998, **123**, 1303–1307.